

Progressive Limb-Aware Virtual Try-On

Xiaoyu Han
Harbin Institute of Technology
Weihai, China
xyhan@stu.hit.edu.cn

Shengping Zhang*
Harbin Institute of Technology
Weihai, China
s.zhang@hit.edu.cn

Qinglin Liu
Harbin Institute of Technology
Weihai, China
qinglin.liu@outlook.com

Zonglin Li
Harbin Institute of Technology
Weihai, China
zonglin.li@hit.edu.cn

Chenyang Wang
Harbin Institute of Technology
Weihai, China
c.wang@stu.hit.edu.cn



Figure 1: Given the human images and in-shop clothing images, our proposed PL-VTON produces high-quality try-on results. In particular, PL-VTON outperforms the state-of-the-art methods in scenes with the complex clothing textures (the first row) and the transformation between long-sleeved and short-sleeved clothing (the second row and the third row).

ABSTRACT

Existing image-based virtual try-on methods directly transfer specific clothing to a human image without utilizing clothing attributes to refine the transferred clothing geometry and textures, which causes incomplete and blurred clothing appearances. In addition, these methods usually mask the limb textures of the input for the clothing-agnostic person representation, which results in inaccurate predictions for human limb regions (i.e., the exposed arm skin),

especially when transforming between long-sleeved and short-sleeved garments. To address these problems, we present a progressive virtual try-on framework, named PL-VTON, which performs pixel-level clothing warping based on multiple attributes of clothing and embeds explicit limb-aware features to generate photo-realistic try-on results. Specifically, we design a Multi-attribute Clothing Warping (MCW) module that adopts a two-stage alignment strategy based on multiple attributes to progressively estimate pixel-level clothing displacements. A Human Parsing Estimator (HPE) is then introduced to semantically divide the person into various regions, which provides structural constraints on the human body and therefore alleviates texture bleeding between clothing and limb regions. Finally, we propose a Limb-aware Texture Fusion (LTF) module to estimate high-quality details in limb regions by fusing textures of the clothing and the human body with the guidance of explicit limb-aware features. Extensive experiments demonstrate that our

*Corresponding author.

proposed method outperforms the state-of-the-art virtual try-on methods both qualitatively and quantitatively. The code is available at <https://github.com/xyhanHIT/PL-VTON>.

CCS CONCEPTS

• **Computing methodologies** → **Computer vision problems**.

KEYWORDS

Virtual Try-on; Image Synthesis; Appearance Flow

ACM Reference Format:

Xiaoyu Han, Shengping Zhang, Qinglin Liu, Zonglin Li, and Chenyang Wang. 2022. Progressive Limb-Aware Virtual Try-On. In *Proceedings of the 30th ACM International Conference on Multimedia (MM '22)*, October 10–14, 2022, Lisboa, Portugal. ACM, New York, NY, USA, 10 pages. <https://doi.org/10.1145/3503161.3547999>

1 INTRODUCTION

Virtual try-on has attracted a lot of attention in recent years because of its wide applications in e-commerce and fashion image editing, which aims to transfer specific clothing to a human image. Existing methods can be roughly classified into 3D-based methods [4, 18, 45, 64] and 2D-based methods [5, 19, 21, 28, 29, 36, 55, 61]. 3D-based methods utilize computer graphics for building 3D models and obtain the result through complex rendering, which has excellent control over the material and the clothing deformation. However, these methods rely heavily on complex data representations and consume massive computational resources. Conversely, 2D-based methods are more suitable for real-world scenarios due to the lightweight data.

The early 2D-based method CA-GAN [29] leverages the generative adversarial network (GAN) to directly generate try-on images without other descriptive person representations, which fails to get photo-realistic results. VITON [21] first proposes the idea of using the thin-plate spline (TPS) transformation to perform clothing warping, which greatly improves the try-on performance. Then CP-VTON [55] adopts an improved TPS transformation with full learnable parameters via a deep convolutional neural network to obtain a more robust result of the clothing alignment. However, each TPS parameter controls the deformation of a coarse pixel block, so these TPS-based methods are limited by the low degrees of freedom, which produce distorted and incorrect results when large geometric deformations occur on the clothing. ClothFlow [19] replaces TPS with the dense pixel-wise appearance flow, but the high degrees of freedom and the lack of proper regularization cause unstable pixel displacements and lead to texture bleeding in the try-on result. We argue that when the estimation of the clothing deformation is constrained by a single stage, the network needs to allocate additional attention to aligning clothing with the human body from other attributes besides the clothing geometry (e.g., the adjustment in spatial location and size), which reduces the finesse and controllability of the clothing warping.

On the other hand, it is difficult to obtain the data of a person wearing different clothing in a fixed pose, so recent methods usually construct the clothing-agnostic person representation to eliminate the effects of the source clothing item and train the network in a self-supervised way. Some of them [2, 10, 66] mask the clothing

regions in the human image along the clothing boundary. However, the rough outline of the clothing is still preserved, which does not keep clothing-agnostic strictly. Others [21, 28, 44, 55, 58] mask the clothing regions and limb regions (i.e., the exposed arm skin in the human image), which loses limb texture information and is negative to the texture retention.

In this paper, we propose PL-VTON to perform stable clothing warping and retain realistic limb textures in the try-on result (as shown in Figure 1), which consists of three progressive modules: (1) Multi-attribute Clothing Warping (MCW), which adopts a two-stage alignment strategy to align the clothing with the human body. In-shop clothing is first adapted in spatial location and size according to the explicit semantic parsing of the paired human image, then a multi-scale flow predictor is used to estimate the geometric deformation of the clothing precisely. (2) Human Parsing Estimator (HPE), which aims to produce the prior guidance for the limb texture extraction and provide structural constraints for the subsequent generation of the try-on result by predicting the parsing map of the person wearing the target clothing. (3) Limb-aware Texture Fusion (LTF), where a coarse-to-fine texture fusion scheme with the limb-aware guidance is applied to preserve high-quality limb textures in the final try-on result.

The contributions of this paper are summarized below:

- We propose a virtual try-on framework named PL-VTON, which generates high-quality try-on results progressively by multi-attribute clothing warping, parsing map estimation, and texture fusion with the limb-aware guidance.
- We design a novel multi-attribute clothing warping module that utilizes a two-stage alignment strategy based on multi-attribute to obtain the fine-grained clothing deformation and warp the clothing precisely.
- We present a novel limb-aware texture fusion module to fuse the textures of the clothing and the human body from coarse to fine, where the explicit limb-aware guidance has a positive impact on the retention of limb details.
- Extensive experiments on the VITON dataset demonstrate the significant superior performance in the image-based virtual try-on task achieved by our PL-VTON.

2 RELATED WORK

2.1 Flow Estimation

Flow estimation aims to find the pixel-level correspondence between two frames or two images. Specifically, it describes which pixels in the source can be used to synthesize the target and how those pixels are transferred to the specific positions in the result. Early flow estimation is usually used in video tasks, which is called optical flow estimation. The optical flow estimation attempts to learn a siamese network by taking two consecutive video frames as the input, then the raw pixels of the first frame are warped to the next one. FlowNet [11] is the first CNN-based end-to-end version for the flow estimation, which uses a U-net architecture to predict the optical flow directly. FlowNet2 [27] adopts the stacked hour-glass network with more training data and more complex training strategies to improve the accuracy in small motion areas. PWC-Net [52] utilizes well-established principles of pyramidal processing, warping, and cost volume processing to predict the optical flow,

which further promotes the performance and reduces the model size simultaneously. RAFT [53] proposes a novel deep network architecture with a recurrent unit, which uses many lightweight and recurrent update operators to estimate the optical flow.

In addition, flow estimation is also applied to predict a 2D vector field without timing information, which warps the source image to the target image based on the similarity in appearance. It is defined as the appearance flow by Zhou et al. [68]. Appearance flow has been widely applied in the field of computer vision. For instance, StructureFlow [46] adopts appearance flow in image inpainting. To generate realistic alternative contents for missing holes, the offset vectors are predicted to flow the pixels from source regions to missing regions. Document image rectification [7, 13, 14, 37, 41, 43] adopts the appearance flow network to regress a dense 2D vector field that samples pixels from the distorted document images to the rectified ones. Appearance flow is also used in human pose transfer, e.g., Li et al. [38] fit a 3D model to the given pose pair and project them back to the 2D plane to compute the dense appearance flow. With the pixel-level displacements, feature warping is performed on the human image and the photo-realistic result of the target pose is generated. In this paper, we adopt the appearance flow to represent the clothing deformation, which acts as the prior information for generating the try-on result.

2.2 Fashion Analysis and Virtual Try-on

Fashion analysis has attracted considerable attention in recent years due to its wide range of applications. The initial focus is more on the classical tasks such as clothing classification [1, 3], clothing recognition [31, 63], clothing segmentation [30, 56, 65], and fashion image retrieval [6, 9, 15, 34]. Recently, more novel tasks such as fashion style estimation [25, 32, 50, 54], clothing recommendation [20, 24, 39, 42, 48, 67], popularity predicting [59], and fashion landmark localization [17, 35, 40, 57, 60] have been explored, where virtual try-on is one of the most challenging visual tasks because it requires both capturing the clothing accurately and merging clothing textures properly with the given human body.

Existing methods for virtual try-on are mainly based on 3D modeling [4, 18, 45, 64] or 2D images [5, 19, 21, 28, 29, 36, 55, 61]. 3D-based methods rely on sophisticated instruments and higher-dimensional calculations to achieve try-on effects, but the complicated process constrains the application value. Conversely, 2D-based methods are more broadly applicable. CA-GAN [29] applies the generative adversarial network (GAN) to learn the relation between the in-shop clothing image and the human image. Based on the relation, the image of the person wearing new clothing is then generalized and generated. VITON [21] proposes a virtual try-on network without using 3D information in any form. It uses thin-plate spline (TPS) transformation to warp the clothing and an encoder-decoder is then used to generate the try-on result. Besides, it adopts a clothing-agnostic person representation to eliminate the effects of the original clothing item in the human image. To improve the accuracy of the warping process, CP-VTON [55] proposes to utilize a deep convolutional neural network to dynamically estimate the TPS parameters. CP-VTON+ [44] is designed based on the pipeline structure of CP-VTON, which corrects the erroneous clothing-agnostic person representation in the dataset and makes

the network input more reasonable. SieveNet [28] further optimizes the clothing warping, where a coarse-to-fine clothing warping network is trained with a novel perceptual geometric matching loss to better model fine intricacies while transforming the target clothing to align with the human body.

However, the above TPS-based methods cannot handle large geometric deformation well due to the limited degrees of freedom. To warp the clothing more freely, some recent methods adopt the appearance flow in their framework. ClothFlow [19] proposes a generative model based on the appearance flow to improve the freedom of clothing deformation. By estimating the dense pixel-level flow between the source and target clothing regions, the model can effectively simulate the geometrical changes and generate the warped clothing image. Nonetheless, due to the unrestricted degrees of deformation and lack of proper regularization, this scheme may lead to drastic and unrealistic clothing warping and cause artifacts or texture bleeding in the final try-on result. Zflow [5] points out the shortcomings of [19] and adopts a gated aggregation of hierarchical flow estimates and some geometric priors as the improvement. PF-AFN [16] proposes a “teacher-tutor-student” knowledge distillation strategy and formulates it as distilling the appearance flows between the clothing image and the human image, which aims to find accurate dense correspondences between them to produce high-quality results. Inspired by the above methods, we use an appearance flow that considers multiple scales to represent the clothing deformation, which is produced by a two-stage alignment strategy progressively. In addition, we adopt the limb-aware guidance to optimize the clothing-agnostic person representation, assisting the network in generating high-quality limb details.

3 METHOD

3.1 Overview

The overview of our proposed progressive limb-aware virtual try-on framework (PL-VTON) is shown in Figure 2, which consists of three modules: Multi-attribute Clothing Warping (MCW), Human Parsing Estimator (HPE), and Limb-aware Texture Fusion (LTF). These modules are cascaded to generate the high-quality virtual try-on result progressively. Specifically, given an in-shop clothing C , an 18-channel keypoint map K , and a 7-channel source parsing map P^s , MCW aims to estimate an aggregated flow f_a , which is applied on C to get a warped clothing C_w . Then HPE uses C_w , K , P^s , and a masked human image I_{mask} to predict a target parsing map P^t , which represents the semantic segmentation of the person wearing the target clothing. Finally, LTF takes C_w , K , P^t , and I_{mask} as the input to first perform the coarse texture fusion and output a coarse try-on result I_c , then a set of limb map patches L_p (obtained through P^t and the human image I) is adopted to refine I_c and get a fine try-on result I_f .

3.2 Multi-attribute Clothing Warping

As illustrated in Figure 2 (a), the proposed Multi-attribute Clothing Warping (MCW) adopts a two-stage alignment strategy: the spatial location and size of the clothing are first adjusted to roughly align the clothing with the human body according to an adaptive circumscribed rectangle, then a multi-scale flow predictor is used

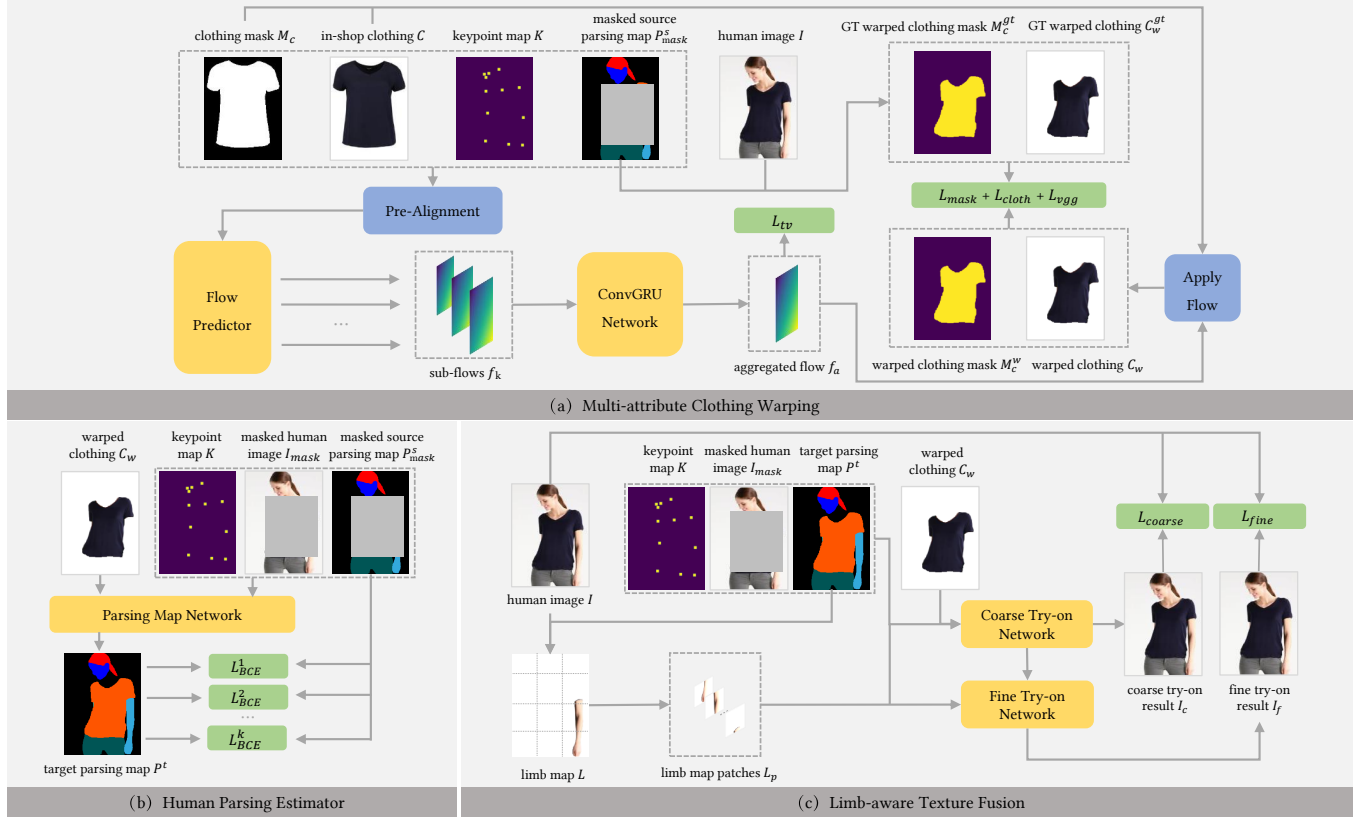


Figure 2: The overview of the proposed PL-VTON. (a) MCW adopts a two-stage alignment strategy to estimate the aggregated flow f_a . (b) HPE estimates the target parsing map P^t to provide structural constraints. (c) LTF first produces the coarse try-on result I_c and then utilizes the information of the limb map to refine I_c and get the fine try-on result I_f .

to estimate the geometric deformation of the clothing precisely and get the warped clothing C_w .

3.2.1 Clothing-agnostic Input. To train the virtual try-on network, a straightforward approach is to leverage the training data of the person wearing different clothing in a fixed pose, which is usually difficult to acquire. It is a good practice to obtain the clothing-agnostic person representation [21] of a human image (i.e., the clothing regions in the human image are masked before entering the network) and send it to the network, so we can treat the human image as both ground truth and input. We apply this representation and further make some improvements for obtaining the prior. We design an adaptive mask scheme, where a circumscribed rectangle of the clothing regions in I is used as the mask (obtained by the extreme values of the clothing pixel position in four directions), and it is modified according to the limb regions (i.e., the exposed arm skin in the human image is added to the masked regions). This mask is used to occlude the source parsing map P^s and the human image I , which ensures that the input does not contain the original clothing information. Note that we do not adopt the human shape map like [21, 28, 44], since it contains the geometric information of the clothing (e.g., the original collar shape) and is not a clothing-agnostic representation strictly, even if it has been down-sampled and interpolated, which is shown in Figure 3.

3.2.2 Pre-alignment in Spatial Location and Size. Generally, the in-shop clothing C and the clothing in I are different in spatial location and size. It is necessary to pre-align the clothing in these two attributes before estimating the appearance flow, which helps the network to handle fine-grained geometric deformation, and the whole warping process becomes more generalizable and controllable because of the separate two-stage alignment strategy.

Therefore, we design an adaptive way to align the in-shop clothing C with the human image I in spatial location and size before geometric deformation. First, for the in-shop clothing mask M_c , we get the center point of its circumscribed rectangle (x_1, y_1) . Similarly, for the clothing regions of I , we get the center point of its circumscribed rectangle (x_2, y_2) . Then a shift operation is performed on the in-shop clothing C with the movement vector $(x_1 - x_2, y_1 - y_2)$ to get the shifted clothing image C_l . Next, the height of the clothing regions in C and I are calculated as h_s and h_t , respectively, and we get a size ratio as h_s/h_t . Note that we do not use the width because some complex human postures seriously affect the horizontal value of the clothing regions in I , which cannot reflect the real size. We use the size ratio h_s/h_t to resize the shifted clothing image C_l and get the resized clothing image C_s .

3.2.3 Multi-scale Flow Predictor. The multi-scale flow predictor aims to produce a set of sub-flows from different scales and

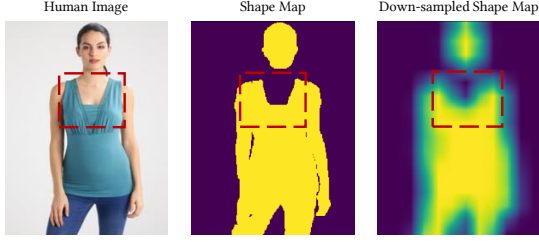


Figure 3: The human shape map contains geometric information of the clothing (e.g., the original collar shape), even if it has been down-sampled and interpolated.

aggregate them into a final precise appearance flow to indicate the geometric deformation of clothing. The backbone network is a ResNet34 [22] with a 5-layer decoder, and its inputs are the resized clothing image $C_s \in \mathbb{R}^{3 \times H \times W}$, the keypoint map $K \in \mathbb{R}^{18 \times H \times W}$ and the source parsing map $P^s \in \mathbb{R}^{7 \times H \times W}$. The k -th layer of the decoder is used to predict the sub-flow $f_k \in \mathbb{R}^{2 \times \frac{H}{6-k} \times \frac{W}{6-k}}$, where $k \in \{1, 2, \dots, 5\}$. Inspired by [5], we adopt a convolution gated recurrent unit (ConvGRU) [49] to aggregate multi-scale sub-flows into a final precise flow, which uses updating and resetting operations to gate these sub-flows and combines them through multiple non-linear weighted summations for the fine-grained deformation.

3.2.4 Loss. We apply the aggregated flow f_a on the in-shop clothing mask M_c to obtain the warped clothing mask M_c^w . This result is used to calculate the mask loss L_{mask} to constrain the clothing geometry, which is formulated as:

$$L_{mask} = \|M_c^w - M_c^{gt}\|_1 \quad (1)$$

where M_c^{gt} is extracted from the source parsing map P^s , it represents the clothing regions in the human image I . Furthermore, M_c^{gt} is also applied to get the clothing C_w^{gt} in the human image, which is regarded as the ground truth of the warped clothing C_w :

$$C_w^{gt} = I \odot M_c^{gt} \quad (2)$$

where \odot is element-wise multiplication. The clothing loss L_{cloth} and the perceptual loss L_{vgg} are formulated as:

$$L_{cloth} = \|C_w - C_w^{gt}\|_1 \quad (3)$$

$$L_{vgg} = \sum_{i=1}^n \lambda_i \|\phi_i(C_w) - \phi_i(C_w^{gt})\|_1 \quad (4)$$

where $\phi_i(\cdot)$ denotes the feature maps of the i -th layer in the visual perception network VGG19 [51] pre-trained on ImageNet [8], and λ_i is the corresponding weight. In addition, a total variation loss [12] is applied to ensure the spatial smoothness for the flow f_a :

$$L_{tv} = \sum_{i \in \Omega} \sqrt{D_x(f_a^i)^2 + D_y(f_a^i)^2} \quad (5)$$

where $D_x(\cdot)$ and $D_y(\cdot)$ are the horizontal and vertical difference functions, respectively. Ω is the area of f_a . Finally, the whole objective function of MCW is presented as:

$$L_{MCW} = \lambda_{mask} L_{mask} + \lambda_{cloth} L_{cloth} + \lambda_{vgg} L_{vgg} + \lambda_{tv} L_{tv} \quad (6)$$

3.3 Human Parsing Estimator

Due to the neglect of structural information, some existing methods [21, 44, 55] suffer from texture bleeding between clothing and human skin, which severely affects the fidelity of final results, especially in the case of the transformation between long-sleeves and short-sleeves. To provide structural constraints for the generation of the try-on result, we adopt Human Parsing Estimator (HPE) to predict the target parsing map, i.e., the semantic segmentation of the person wearing the target clothing. In addition, the second role of the parsing map is to extract limb textures from the human image I , which is the premise of the follow-up limb-aware guidance.

Figure 2 (b) illustrates the schematic of Human Parsing Estimator (HPE). Given the warped clothing C_w , the keypoint map K , and the masked source parsing map P_{mask}^s , this module aims to generate the target parsing map P^t . The network consists of an encoder to extract the features from the original human image and a decoder to output the target parsing result. We add an additional squeeze-and-excitation (SE) block [26] during downsampling to assign the weight to each channel item of the input and feature maps, which adapts its effect on the final generated image. HPE is trained with a weighted cross-entropy loss, which is formulated as:

$$L_{HPE} = -\frac{1}{n} \sum_{i=0}^n \sum_{j=0}^c w_j P_{i,j}^s \log(P_{i,j}^t) \quad (7)$$

where n is the sample numbers, c is the number of channels of P^s and P^t , and w_j is the weight for the j -th channel. Note that we increase the weights of the clothing and limb classes to better prevent the pixels of skin from bleeding into other regions.

3.4 Limb-aware Texture Fusion

After obtaining the warped clothing C_w aligned with the human body from Multi-attribute Clothing Warping and the parsing map P^t of the person wearing the target clothing from Human Parsing Estimator, the final goal is to generate the try-on result by fusing textures of C_w and I according to P^t . We observe existing methods usually generate limb regions with the wrong shape and color due to the discarding of necessary texture information of the input. Conversely, our Limb-aware Texture Fusion (LTF) module takes full advantage of the limb textures from the human image I to produce realistic limb details. Furthermore, our limb-aware guidance makes the network better handle the transformation of the clothing categories between long-sleeved and short-sleeved. LTF consists of two stages: (1) predicting the coarse try-on result I_c and (2) using limb map patches L_p to refine I_c and get the fine try-on result I_f .

3.4.1 Coarse Try-on. The first stage of LTF aims to fuse textures of the warped clothing and the human body roughly to generate the appearance of clothing regions and other regions where textures are easily transferred (e.g., face, hair, and pants). Although limb textures are also generated, there are some inaccuracies in details since the limb guidance has not been added, which are optimized in the next stage. Given the warped clothing C_w , the keypoint map K , the target parsing map P^t , and the masked human image I_{mask} , an encoder-decoder network produces the coarse try-on result I_c . Each input has its role: the warped clothing C_w provides clothing textures, the keypoint map K ensures the human posture

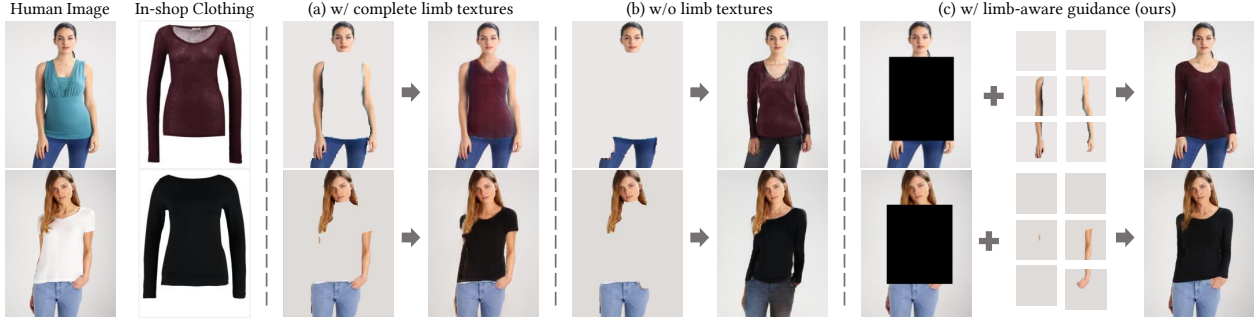


Figure 4: The effect of the amount of limb information used to produce the try-on result.

is consistent with the original image, the target parsing map P^t provides the structural constraints for the generated human body, and the masked human image I_{mask} offers textures of other regions (e.g., face, hair, and pants) that need to be preserved.

3.4.2 Limb-aware Refinement. Experiments have demonstrated the network can utilize source limb textures to generate the result similar to the original image (as shown in Figure 4 (a)). We train our network in a self-supervised way and try to make the virtual try-on result become exactly the same as the original human image during the training process. However, it is not what we expected that this still occurs in the test set, which means that too much information from the source space causes the network to converge to a local optimum in the training set. This problem is especially serious when the clothing category changes during virtual try-on. For example, we try to change the short-sleeved garment in the human image to a long-sleeved one, it easily fails when the network receives the complete limb textures from the original human image, as shown in Figure 4 (a), the wrong results only transfer the clothing textures but ignore the clothing geometry. We argue the reason for this is that the rough outline of the clothing is still preserved when complete limb textures are obtained by masking the clothing along the border, which does not keep clothing-agnostic strictly. Therefore, we need to discard part of limb textures to mask the geometric appearance of the clothing. Nonetheless, as shown in the examples in Figure 4 (b) and (c), the limb textures are necessary as the auxiliary information, which effectively alleviates artifacts and distortions in the results and preserves the realistic limb details.

In order to properly utilize the guidance of the limb textures while keeping clothing-agnostic for training, we adopt the limb map patches to shield the geometric information and fuse the limb textures into the coarse try-on result I_c to obtain the fine try-on result I_f . Figure 2 (c) illustrates the overview of the Limb-aware Texture Fusion (LTF) module. First, the limb map L is obtained by the masking operation of the target parsing map P^t and the human image I . Then, we divide L into patches $L_p \in \mathbb{R}^{\frac{H}{s} \times \frac{W}{s}}$, where s represents the patch scale. L_p items are concatenated in the channel dimension and fed into the fine try-on network with K , I_{mask} , P^t , and I_c . The fine try-on network is also a U-shaped structure with a ResNet34 and 5 decoder layers. Note that we blur the limb regions of I_c before it enters the network to narrow the gap between the training set and testing set. The blurring operation

is only applied during training, which is omitted in the evaluation stage to enhance the quality of the try-on result.

3.4.3 Loss. The total loss of this module is defined as $L_{LTF} = L_c + L_f$, where L_c is the loss of the coarse stage and L_f is the loss of the fine stage. Each of items both contains the mean absolute error L_1 , the perceptual loss L_{vgg} , and the edge loss L_{edge} . Note that we use L_{edge} based on Sobel filters (∇_x, ∇_y) to correct the horizontal and vertical gradients, which improves the smoothness of the reconstructed textures. L_c is defined as:

$$L_c = \lambda_{img} \|I_c - I\|_1 + \lambda_p \|\phi_i(I_c) - \phi_i(I)\|_1 + \lambda_{edge} \|\psi(I_c) - \psi(I)\|_1 \quad (8)$$

where $\phi_i(\cdot)$ represents the feature maps extracted from the i -th layer of the VGG19 network. $\psi(\cdot)$ denotes the gradients extracted by Sobel filters. Similarly, L_f is defined as:

$$L_f = \lambda_{img} \|I_f - I\|_1 + \lambda_p \|\phi_i(I_f) - \phi_i(I)\|_1 + \lambda_{edge} \|\psi(I_f) - \psi(I)\|_1 \quad (9)$$

4 EXPERIMENT

In this section, we evaluate our PL-VTON on the VITON [21] dataset. We first introduce the VITON dataset and show the implementation details, which include the training details and the hyperparameter settings. Then, we compare PL-VTON with the state-of-the-art methods both quantitatively and qualitatively, including CP-VTON [55], CP-VTON+ [44], ACGPN [62], and PFAFN [16]. Finally, we perform ablation studies to analyze the effectiveness of each proposed contribution of PL-VTON.

4.1 Dataset

We use the VITON [21] dataset to ensure the consistency of baseline methods. The dataset contains 19K image pairs, each pair consists of a human image and a corresponding in-shop clothing image, and the size of all images is 256×192 . After removing the mislabeled data, there are still 16K image pairs remaining, 1/8 of which are used for testing and the others are used for training.

4.2 Implementation Details

Our PL-VTON is implemented with Pytorch on an RTX 3090 GPU and we train three modules independently. Specifically, we first train MCW for 24K steps with batch size 16, where the loss weights $\lambda_{mask} = 2.5$, $\lambda_{cloth} = 5$, $\lambda_{vgg} = 1$, and $\lambda_{tv} = 0.1$. Then we train HPE for 40K steps with batch size of 16, where $w_0 = w_1 = w_2 = w_6 = 1$ and $w_3 = w_4 = w_5 = 3$. Finally, we train LTF for 80K steps with



Figure 5: Visual comparisons of five different methods. PL-VTON works well for the transformation between long and short sleeves (the first row), fancy clothing try-on (the second row), cognition of the collar and hem (the third row), clothing texture transfer (the fourth row), and limb detail retention (the last row).

batch size of 4, where $\lambda_{img} = 1$, $\lambda_p = 2$, and $\lambda_{edge} = 0.1$. Adam [33] optimizer is used with $\beta_1 = 0.5$ and $\beta_2 = 0.999$ in both stages. Learning rate is fixed at 0.0001 in the first half of training and then linearly decays to zero for the remaining steps.

4.3 Qualitative Results

We perform visual comparisons of CP-VTON [55], CP-VTON+ [44], ACGPN [62], PF-AFN [16], and our PL-VTON. As shown in Figure 5, where some disadvantages are highlighted with red boxes. In the first row, we compare the quality of try-on results when the clothing category changes (i.e., the transformation between long-sleeved and short-sleeved clothing). Most existing methods do not handle the changes in the sleeve length well, and there are more artifacts in the cuff regions. In the second row, we show the ability of methods to handle fancy clothing. Fancy clothing generally has unusual silhouettes and textures, which is extremely challenging in the virtual try-on. It can be seen that most existing methods cannot completely transfer the fancy clothing to the human body, there are some inaccurate clothing deformation and clothing texture missing in the red boxes. In the third row, we aim to demonstrate the cognitive ability of these methods for clothing structure. Except for our PL-VTON, other methods both have some cognitive errors, especially for the collar and hem, which are easily mistaken for the front of the clothing. The fourth row compares the ability of clothing texture transfer. Some distortions appear in the results of CP-VTON, CP-VTON+, and PF-AFN, and the textures preserved by ACPGN are incomplete. In the last row, we examine the ability of methods

Table 1: Quantitative evaluation results and user study results of existing methods and our PL-VTON. PL-VTON* is PL-VTON without the two-stage alignment strategy, and PL-VTON[†] is PL-VTON without the limb-aware guidance. For the percentage results a/b in the third column, a is the percentage that the compared method is considered better than our PL-VTON, and b is the percentage that our PL-VTON is considered better than the compared method.

Method	FID	Human
CP-VTON [55]	19.88	21.70% / 78.30%
CP-VTON+ [44]	16.27	16.67% / 83.33%
ACGPN [62]	12.69	24.44% / 75.56%
PF-AFN [16]	12.81	23.45% / 76.55%
PL-VTON*	12.43	-
PL-VTON [†]	12.58	-
PL-VTON (ours)	12.16	reference

to preserve limb details. For CP-VTON and CP-VTON+, there is severe blurring on the fingers, and the color tone of the generated images is different from the original. The results of ACGPN have some distortions in the finger and forearm regions. PF-AFN and PL-VTON achieve the better performance to maintain the non-clothing characteristics, but the former generates incorrect textures where the limb and clothing meet.

The above qualitative experiments show that our PL-VTON can better handle cross-category clothing transfer and fancy clothing

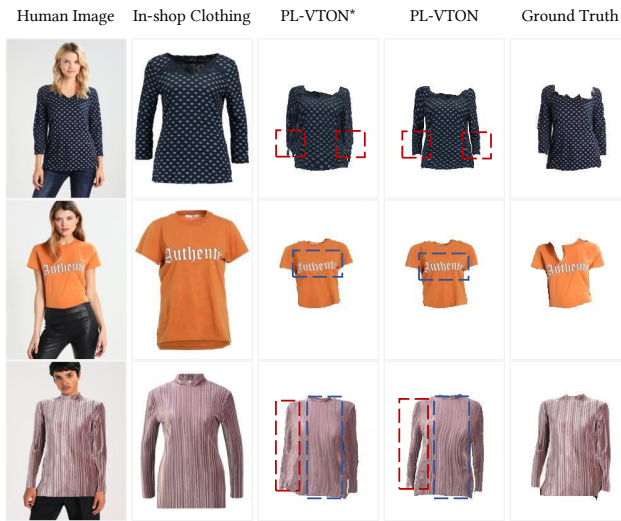


Figure 6: The ablation study of the proposed two-stage alignment strategy in Multi-attribute Clothing Warping (MCW), where red boxes focus on the clothing shape and blue boxes focus on the clothing textures. PL-VTON* is PL-VTON without the two-stage alignment strategy.

transfer, and it is able to preserve realistic limb details while generating more accurate clothing textures.

4.4 Quantitative Results

We adopt Fréchet Inception Distance (FID) [23] to measure the feature vector distance between the real image and the generated try-on result. The higher quality of the result gets a lower score of FID. Note that Inception Score (IS) is abandoned because Rosca et.al [47] have demonstrated that there are misleading results when IS is applied to the model trained on the datasets other than ImageNet. Table 1 summarizes the FID scores of CP-VTON [55], CP-VTON+ [44], ACGPN [62], PF-AFN [16], and our PL-VTON on the VITON dataset. Obviously, PL-VTON achieves a significantly better FID of 12.16 compared to the second best value 12.69.

4.5 User Study

The A/B test is conducted to further evaluate the results of our method. We perform four pairwise comparisons and each comparison consists of 50 image pairs of PL-VTON and another baseline method. 50 volunteers are asked to consider the quality of these try-on images and choose the better one. The results are summarized in Table 1, which demonstrate that PL-VTON always gives a relatively better visual experience than other existing methods with a much higher percentage. These random and subjective tests further corroborate previous evaluation results, showing that our method significantly outperforms other methods.

4.6 Ablation Studies

We present ablation studies on the test data to verify the role and effectiveness of the two-stage alignment strategy and the limb-aware guidance. First, we use PL-VTON* to indicate PL-VTON



Figure 7: The ablation study of the limb-aware guidance in Limb-aware Texture Fusion (LTF). PL-VTON† represents that the limb-aware guidance is removed from PL-VTON.

without the alignment in spatial location and size, which takes in-shop clothing C as the input and directly estimates the appearance flow by a deep convolutional neural network. Then we use PL-VTON† to denote that the limb-aware guidance is removed from the network of Limb-aware Texture Fusion, and the virtual try-on result is produced by a single stage. Figure 6 shows the visual comparisons between PL-VTON* and PL-VTON, where red boxes focus on the clothing geometry and blue boxes focus on the clothing textures. It can be seen that compared with PL-VTON, the results of PL-VTON* have some wrong shape problems in the sleeve and cuff regions (the first row and the third row) and some blurred textures (the second row and the third row). PL-VTON† and PL-VTON are compared in Figure 7, which shows the limb regions generated by PL-VTON† have some distortions while the results of full PL-VTON are more realistic and accurate. The quantitative comparisons of PL-VTON*, PL-VTON†, and PL-VTON are also shown in Table 1, which indicate that the FID metric increases after removing the two-stage alignment strategy or the limb-aware guidance from PL-VTON, but the performance is still better than other methods.

5 CONCLUSION

In this paper, we propose a novel progressive limb-aware virtual try-on framework named PL-VTON. PL-VTON consists of Multi-attribute Clothing Warping (MCW), Human Parsing Estimator (HPE), and Limb-aware Texture Fusion (LTF), which produces stable clothing deformation and handles the texture retention well in the final try-on result. Extensive experiments show great superiority of PL-VTON over the state-of-the-art virtual try-on methods both qualitatively and quantitatively.

ACKNOWLEDGMENTS

This work was supported by the National Natural Science Foundation of China (No. 61872112) and the Taishan Scholars Program of Shandong Province (No. tsqn201812106).

REFERENCES

- [1] Lukas Bossard, Matthias Dantone, Christian Leistner, Christian Wengert, Till Quack, and Luc Van Gool. 2012. Apparel Classification with Style. In *ACCV*. 321–335.
- [2] Chieh-Yun Chen, Ling Lo, Pin-Jui Huang, Hong-Han Shuai, and Wen-Huang Cheng. 2021. FashionMirror: Co-Attention Feature-Remapping Virtual Try-On With Sequential Template Poses. In *ICCV*. 13809–13818.
- [3] Huizhong Chen, Andrew Gallagher, and Bernd Girod. 2012. Describing Clothing by Semantic Attributes. In *ECCV*. 609–623.
- [4] Wenzheng Chen, Huan Wang, Yangyan Li, Hao Su, Zhenhua Wang, Changhe Tu, Dani Lischinski, Daniel Cohen-Or, and Baoquan Chen. 2016. Synthesizing Training Images for Boosting Human 3D Pose Estimation. In *3DV*. 479–488.
- [5] Ayush Chopra, Rishabh Jain, Mayur Hemani, and Balaji Krishnamurthy. 2021. ZFlow: Gated Appearance Flow-based Virtual Try-on with 3D Priors. In *ICCV*. 5433–5442.
- [6] Charles Corbiere, Hedi Ben-Younes, Alexandre Ramé, and Charles Ollion. 2017. Leveraging Weakly Annotated Data for Fashion Image Retrieval and Label Prediction. In *ICCVW*. 2268–2274.
- [7] Sagnik Das, Ke Ma, Zhixin Shu, Dimitris Samaras, and Roy Shilkrot. 2019. DewarpNet: Single-Image Document Unwarping With Stacked 3D and 2D Regression Networks. In *ICCV*. 131–140.
- [8] Jia Deng, Wei Dong, Richard Socher, Li-Jia Li, Kai Li, and Li Fei-Fei. 2009. ImageNet: A Large-Scale Hierarchical Image Database. In *CVPR*. 248–255.
- [9] Antonio D’Innocente, Nikhil Garg, Yuan Zhang, Loris Bazzani, and Michael Donoser. 2021. Localized Triplet Loss for Fine-grained Fashion Image Retrieval. In *CVPR*. 3910–3915.
- [10] Haoye Dong, Xiaodan Liang, Xiaohui Shen, Bochao Wang, Hanjiang Lai, Jia Zhu, Zhiting Hu, and Jian Yin. 2019. Towards Multi-pose Guided Virtual Try-on Network. In *ICCV*. 9026–9035.
- [11] Alexey Dosovitskiy, Philipp Fischer, Eddy Ilg, Philip Hausser, Caner Hazirbas, Vladimir Golkov, Patrick Van Der Smagt, Daniel Cremers, and Thomas Brox. 2015. FlowNet: Learning Optical Flow with Convolutional Networks. In *ICCV*. 2758–2766.
- [12] Lijie Fan, Wenbing Huang, Chuang Gan, Stefano Ermon, Boqing Gong, and Junzhou Huang. 2018. End-to-End Learning of Motion Representation for Video Understanding. In *CVPR*. 6016–6025.
- [13] Hao Feng, Yuechen Wang, Wengang Zhou, Jiajun Deng, and Houqiang Li. 2021. DocTr: Document Image Transformer for Geometric Unwarping and Illumination Correction. *arXiv preprint arXiv:2110.12942* (2021).
- [14] Hao Feng, Wengang Zhou, Jiajun Deng, Qi Tian, and Houqiang Li. 2021. DocScanner: Robust Document Image Rectification with Progressive Learning. *arXiv preprint arXiv:2110.14968* (2021).
- [15] Bojana Gajic and Ramon Baldrich. 2018. Cross-Domain Fashion Image Retrieval. In *CVPRW*. 1869–1871.
- [16] Yuying Ge, Yibing Song, Ruimao Zhang, Chongjian Ge, Wei Liu, and Ping Luo. 2021. Parser-Free Virtual Try-on via Distilling Appearance Flows. In *CVPR*. 8485–8493.
- [17] Yuying Ge, Ruimao Zhang, Xiaogang Wang, Xiaoou Tang, and Ping Luo. 2019. DeepFashion2: A Versatile Benchmark for Detection, Pose Estimation, Segmentation and Re-Identification of Clothing Images. In *CVPR*. 5337–5345.
- [18] Peng Guan, Loretta Reiss, David A Hirshberg, Alexander Weiss, and Michael J Black. 2012. DRAPE: Dressing Any Person. *ACM TOG* 31, 4 (2012), 1–10.
- [19] Xintong Han, Xiaojun Hu, Weilin Huang, and Matthew R Scott. 2019. ClothFlow: A Flow-Based Model for Clothed Person Generation. In *ICCV*. 10471–10480.
- [20] Xintong Han, Zuxuan Wu, Yu-Gang Jiang, and Larry S Davis. 2017. Learning Fashion Compatibility with Bidirectional LSTMs. In *ACM MM*. 1078–1086.
- [21] Xintong Han, Zuxuan Wu, Zhe Wu, Ruichi Yu, and Larry S Davis. 2018. VITON: An Image-based Virtual Try-on Network. In *CVPR*. 7543–7552.
- [22] Kaiming He, Xiangyu Zhang, Shaoqing Ren, and Jian Sun. 2016. Deep Residual Learning for Image Recognition. In *CVPR*. 770–778.
- [23] Martin Heusel, Hubert Ramsauer, Thomas Unterthiner, Bernhard Nessler, and Sepp Hochreiter. 2017. GANs Trained by a Two Time-Scale Update Rule Converge to a Local Nash Equilibrium. *NeurIPS* 30 (2017), 6626–6637.
- [24] Shintami Chusnul Hidayati, Cheng-Chun Hsu, Yu-Ting Chang, Kai-Lung Hua, Jianlong Fu, and Wen-Huang Cheng. 2018. What Dress Fits Me Best? Fashion Recommendation on the Clothing Style for Personal Body Shape. In *ACM MM*. 438–446.
- [25] Wei-Lin Hsiao and Kristen Grauman. 2017. Learning the Latent “Look”: Unsupervised Discovery of a Style-Coherent Embedding from Fashion Images. In *ICCV*. 4203–4212.
- [26] Jie Hu, Li Shen, and Gang Sun. 2018. Squeeze-and-Excitation Networks. In *CVPR*. 7132–7141.
- [27] Eddy Ilg, Nikolaus Mayer, Tonmoy Saikia, Margret Keuper, Alexey Dosovitskiy, and Thomas Brox. 2017. FlowNet 2.0: Evolution of Optical Flow Estimation with Deep Networks. In *CVPR*. 2462–2470.
- [28] Sargan Jandial, Ayush Chopra, Kumar Ayush, Mayur Hemani, Balaji Krishnamurthy, and Abhijeet Halwai. 2020. SieveNet: A Unified Framework for Robust Image-Based Virtual Try-On. In *WACV*. 2182–2190.
- [29] Nikolay Jetchev and Urs Bergmann. 2017. The Conditional Analogy GAN: Swapping Fashion Articles on People Images. In *ICCVW*. 2287–2292.
- [30] Wei Ji, Xi Li, Yueting Zhuang, Omar El Farouk Bourahla, Yixin Ji, Shihao Li, and Jiabao Cui. 2018. Semantic Locality-Aware Deformable Network for Clothing Segmentation. In *IJCAL*. 764–770.
- [31] Yannis Kalantidis, Lyndon Kennedy, and Li-Jia Li. 2013. Getting the Look: Clothing Recognition and Segmentation for Automatic Product Suggestions in Everyday Photos. In *ICMR*. 105–112.
- [32] M Hadi Kiapour, Kota Yamaguchi, Alexander C Berg, and Tamara L Berg. 2014. Hipster Wars: Discovering Elements of Fashion Styles. In *ECCV*. 472–488.
- [33] Diederik P Kingma and Jimmy Ba. 2014. Adam: A Method for Stochastic Optimization. *arXiv preprint arXiv:1412.6980* (2014).
- [34] Yining Liang, Yuan He, Fan Yang, Jianfeng Dong, and Hui Xue. 2020. Which Is Plagiarism: Fashion Image Retrieval Based on Regional Representation for Design Protection. In *CVPR*. 2595–2604.
- [35] Sumin Lee, Sungchan Oh, Chanho Jung, and Changick Kim. 2019. A Global-Local Embedding Module for Fashion Landmark Detection. In *ICCVW*. 3153–3156.
- [36] Kedan Li, Min Jin Chong, Jeffrey Zhang, and Jingen Liu. 2021. Toward Accurate and Realistic Outfits Visualization with Attention to Details. In *CVPR*. 15546–15555.
- [37] Xiaoyu Li, Bo Zhang, Jing Liao, and Pedro V Sander. 2019. Document Rectification and Illumination Correction Using a Patch-Based CNN. *ACM TOG* 38, 6 (2019), 1–11.
- [38] Yining Li, Chen Huang, and Chen Change Loy. 2019. Dense Intrinsic Appearance Flow for Human Pose Transfer. In *CVPR*. 3693–3702.
- [39] Ziwei Liu, Ping Luo, Shi Qiu, Xiaogang Wang, and Xiaoou Tang. 2016. DeepFashion: Powering Robust Clothes Recognition and Retrieval with Rich Annotations. In *CVPR*. 1096–1104.
- [40] Ziwei Liu, Sijie Yan, Ping Luo, Xiaogang Wang, and Xiaoou Tang. 2016. Fashion Landmark Detection in the Wild. In *ECCV*. 229–245.
- [41] Ke Ma, Zhixin Shu, Xue Bai, Jue Wang, and Dimitris Samaras. 2018. DocUNet: Document Image Unwarping via a Stacked U-Net. In *CVPR*. 4700–4709.
- [42] Yihui Ma, Jia Jia, Suping Zhou, Jingtian Fu, Yejun Liu, and Zijian Tong. 2017. Towards Better Understanding the Clothing Fashion Styles: A Multimodal Deep Learning Approach. In *AAAI*. 38–44.
- [43] Amir Markovitz, Inbal Lavi, Or Perel, Shai Mazon, and Roei Litman. 2020. Can You Read Me Now? Content Aware Rectification Using Angle Supervision. In *ECCV*. 208–223.
- [44] Matiur Rahman Minar, Thai Thanh Tuan, Heejune Ahn, Paul Rosin, and Yu-Kun Lai. 2020. CP-VTON+: Clothing Shape and Texture Preserving Image-Based Virtual Try-On. In *CVPRW*.
- [45] Gerard Pons-Moll, Sergi Pujades, Sonny Hu, and Michael J Black. 2017. ClothCap: Seamless 4D Clothing Capture and Retargeting. *ACM TOG* 36, 4 (2017), 1–15.
- [46] Yurui Ren, Xiaoming Yu, Ruonan Zhang, Thomas H Li, Shan Liu, and Ge Li. 2019. StructureFlow: Image Inpainting via Structure-Aware Appearance Flow. In *ICCV*. 181–190.
- [47] Mihaela Rosca, Balaji Lakshminarayanan, David Warde-Farley, and Shakir Mohamed. 2017. Variational Approaches for Auto-Encoding Generative Adversarial Networks. *arXiv preprint arXiv:1706.04987* (2017).
- [48] Dandan Sha, Daling Wang, Xiangmin Zhou, Shi Feng, Yifei Zhang, and Ge Yu. 2016. An Approach for Clothing Recommendation Based on Multiple Image Attributes. In *WAIM*. 272–285.
- [49] Mennatullah Siam, Sepehr Valipour, Martin Jagersand, and Nilanjan Ray. 2017. Convolutional gated recurrent networks for video segmentation. In *ICIP*. 3090–3094.
- [50] Edgar Simo-Serra and Hiroshi Ishikawa. 2016. Fashion Style in 128 Floats: Joint Ranking and Classification Using Weak Data for Feature Extraction. In *CVPR*. 298–307.
- [51] Karen Simonyan and Andrew Zisserman. 2014. Very Deep Convolutional Networks for Large-Scale Image Recognition. *arXiv preprint arXiv:1409.1556* (2014).
- [52] Deqing Sun, Xiaodong Yang, Ming-Yu Liu, and Jan Kautz. 2018. PWC-Net: CNNs for Optical Flow Using Pyramid, Warping, and Cost Volume. In *CVPR*. 8934–8943.
- [53] Zachary Teed and Jia Deng. 2020. RAFT: Recurrent All-Pairs Field Transforms for Optical Flow. In *ECCV*. 402–419.
- [54] Andreas Veit, Balazs Kovacs, Sean Bell, Julian McAuley, Kavita Bala, and Serge Belongie. 2015. Learning Visual Clothing Style with Heterogeneous Dyadic Co-Occurrences. In *ICCV*. 4642–4650.
- [55] Bochao Wang, Huabin Zheng, Xiaodan Liang, Yimin Chen, Liang Lin, and Meng Yang. 2018. Toward Characteristic-Preserving Image-Based Virtual Try-On Network. In *ECCV*. 589–604.
- [56] Nan Wang and Haizhou Ai. 2011. Who Blocks Who: Simultaneous Clothing Segmentation for Grouping Images. In *ICCV*. 1535–1542.
- [57] Wenguan Wang, Yuanlu Xu, Jianbing Shen, and Song-Chun Zhu. 2018. Attentive Fashion Grammar Network for Fashion Landmark Detection and Clothing Category Classification. In *CVPR*. 4271–4280.
- [58] Zhenyu Xie, Zaiyu Huang, Fuwei Zhao, Haoye Dong, Michael Kampffmeyer, and Xiaodan Liang. 2021. Towards Scalable Unpaired Virtual Try-On via Patch-Routed

- Spatially-Adaptive GAN. *NeurIPS* 34 (2021), 2598–2610.
- [59] Kota Yamaguchi, Tamara L Berg, and Luis E Ortiz. 2014. Chic or Social: Visual Popularity Analysis in Online Fashion Networks. In *ACM MM*. 773–776.
- [60] Sijie Yan, Ziwei Liu, Ping Luo, Shi Qiu, Xiaogang Wang, and Xiaoou Tang. 2017. Unconstrained Fashion Landmark Detection via Hierarchical Recurrent Transformer Networks. In *ACM MM*. 172–180.
- [61] Fan Yang and Guosheng Lin. 2021. CT-Net: Complementary Transferring Network for Garment Transfer With Arbitrary Geometric Changes. In *CVPR*. 9899–9908.
- [62] Han Yang, Ruimao Zhang, Xiaobao Guo, Wei Liu, Wangmeng Zuo, and Ping Luo. 2020. Towards Photo-Realistic Virtual Try-On by Adaptively Generating-Preserving Image Content. In *CVPR*. 7850–7859.
- [63] Ming Yang and Kai Yu. 2011. Real-time clothing recognition in surveillance videos. In *ICIP*. 2937–2940.
- [64] Shan Yang, Tanya Ambert, Zherong Pan, Ke Wang, Licheng Yu, Tamara Berg, and Ming C Lin. 2016. Detailed Garment Recovery from a Single-View Image. *arXiv preprint arXiv:1608.01250* (2016).
- [65] Wei Yang, Ping Luo, and Liang Lin. 2014. Clothing Co-Parsing by Joint Image Segmentation and Labeling. In *CVPR*. 3182–3189.
- [66] Ruiyun Yu, Xiaoqi Wang, and Xiaohui Xie. 2019. VTNFP: An Image-Based Virtual Try-On Network With Body and Clothing Feature Preservation. In *ICCV*. 10511–10520.
- [67] Wenhui Yu, Huidi Zhang, Xiangnan He, Xu Chen, Li Xiong, and Zheng Qin. 2018. Aesthetic-Based Clothing Recommendation. In *WWW*. 649–658.
- [68] Tinghui Zhou, Shubham Tulsiani, Weilun Sun, Jitendra Malik, and Alexei A Efros. 2016. View Synthesis by Appearance Flow. In *ECCV*. 286–301.